Japanese Journal of Physiology, **30**, 841–857, 1980

Reconstruction of Sino-atrial Node Pacemaker Potential Based on the Voltage Clamp Experiments

Kaoru YANAGIHARA, Akinori NOMA, and Hiroshi IRISAWA

National Institute for Physiological Science, Myodaiji, Okazaki, 444 Japan

Abstract The pacemaker activity of the S-A node cell was explained by reconstructing the pacemaker potential using a Hodgkin-Huxley type mathematical model which was based on the reported voltage clamp data. In this model four dynamic currents, the sodium current, i_{Na}, the slow inward current, i_s, the potassium current, i_K, and the hyperpolarization-activated current, i_h, in addition to a time-independent leak current, i_1 were included. The model simulated the spontaneous action potential the current voltage relationship, and the voltage clamp experiment in normal Tyrode solution of the rabbit S-A node. Furthermore, the changes of activity induced by the potassium current blocker Ba^{2+}, by applying constant current, acetylcholine, and epinephrine were also reconstructed.

It was strongly suggested that the pacemaker depolarization in the S-A node cell is mainly due to a gradual increase of i_s during diastole, and that the contribution of i_K is much less compared to the potassium current i_{K_2} in the Purkinje fiber pacemaker depolarization. The rising phase of the action potential was due to i_s and the plateau phase is determined by both the inactivation of i_s and activation of i_K.

Automatic excitation is one of the characteristic features of the myocardium. This property is solely attributable to the pacemaker activity of the sino-atrial node (S-A node) cells in the intact heart, although other myocardia can also initiate a spontaneous action potential under various experimental, as well as pathological conditions.

Spontaneously beating cells are characterized by having a slow diastolic depolarization (DRAPER and WEIDMANN, 1951; TRAUTWEIN and ZINK, 1952; WEST, 1955). Ionic mechanisms underlying pacemaker depolarization have been extensively studied by voltage clamp experiments, and the result has always shown a gradual decay of K conductance on repolarization after a depolarizing clamp pulse. Pacemaker depolarization generated mainly by a spontaneous decrease of K conductance is confirmed in the mathematical model of cardiac excitation

Received for publication June 2, 1980
柳原　薫，野間昭典，入沢　宏

(McAllister *et al.*, 1975; Beeler and Reuter, 1977).

When the K current was reconstructed during the diastole in the S-A node, however, it was found that the change of K current during the pacemaker potential is much smaller compared to i_{K_2} in the Purkinje fiber. In agreement with this fact the pacemaker depolarization was generated even by applying a constant outward current to the S-A node cells whose time-dependent K current was blocked by Ba ion (Yanagihara and Irisawa, 1980). Furthermore, the chronotropic action of epinephrine could be explained only by assuming a contribution of the slow inward current to the diastolic depolarization (Noma *et al.*, 1980). The inward current system generating the rising phase of the action potential is the slow inward current in the S-A node, while in the Purkinje fiber and in the ventricular fiber it is the sodium current (Weidmann, 1955). These findings indicate that the mechanisms of pacemaker activity of the S-A node cell appear quite different from those in the Purkinje fiber and ventricular fiber. Therefore, in order to clarify the ionic mechanism of the pacemaker activity of the S-A node cell it is necessary to construct a model based on information of the S-A node, which is now sufficiently available from voltage clamp experiments on the mammalian S-A node (for review, Irisawa, 1978) and from the frog sinus venosus (Brown *et al.*, 1977). In the present study, a model simulating the electrical responses of the S-A node cell to various experimental conditions was reconstructed using the Hodgkin-Huxley type formulation of the membrane current.

METHODS

The general form of equations describing the time- and voltage-dependent current component is (Hodgkin and Huxley, 1952; Noble and Tsien, 1968),

$$i=y\cdot\bar{i}\,, \tag{1}$$

where $\bar{i}$ is the product of the driving force and the limiting conductance. The latter is a function of the membrane potential in the slow inward current and the potassium current. y is the gating variable and follows first-order kinetics,

$$dy/dt=\alpha_y(1-y)-\beta_y\cdot y\,. \tag{2}$$

The variable y takes a value between 0 and 1. α_y and β_y denote the rate constants of opening and closing of the ionic channel. In the rabbit S-A node, four dynamic current systems were dissected from the recorded membrane current; a slow inward current, i_s, sodium current, i_{Na}, delayed inward current activated by hyperpolarization, i_h, and the potassium current, i_K. In addition to these dynamic currents a time-independent leak current was incorporated in the S-A node membrane model. The unit membrane was modelled as a capacitance of 1 μF (C_m) connected in parallel to five different ionic channels. Mathematically, this equivalent circuit is expressed by the following equation,

$$C_m\cdot dE/dt=i_m-(i_s+i_{Na}+i_K+i_h+i_l)\,, \tag{3}$$

where E is the membrane potential and i_m is the total current passing through the unit membrane. The current components are described by the following equations, where the rate constants are given in $msec^{-1}$ and the membrane potential in mV.

1) $i_s=(0.95d+0.05)\cdot(0.95f+0.05)\cdot\bar{i}_s$ (4)

$$\alpha_d=\frac{1.045\times10^{-2}(E+35)}{1-\exp(-(E+35)/2.5)}+\frac{3.125\times10^{-2}E}{1-\exp(-E/4.8)} \tag{5}$$

$$\beta_d=\frac{4.21\times10^{-3}(E-5)}{\exp((E-5)/2.5)-1} \tag{6}$$

$$\alpha_f=\frac{3.55\times10^{-4}(E+20)}{\exp((E+20)/5.633)-1} \tag{7}$$

$$\beta_f=\frac{9.44\times10^{-4}|E+60|}{1+\exp(-(E+29.5)/4.16)} \tag{8}$$

$$\bar{i}_s=12.5(\exp(E-30)/15)-1) \tag{9}$$

2) $i_{Na}=m^3\cdot h\cdot\bar{i}_{Na}$ (10)

$$\alpha_m=\frac{E+37}{1-\exp(-(E+37)/10)} \tag{11}$$

$$\beta_m=40\exp(-5.6\times10^{-2}(E+62)) \tag{12}$$

$$\alpha_h=1.209\times10^{-3}\exp(-(E+20)/6.534) \tag{13}$$

$$\beta_h=\frac{1}{\exp(-(E+30)/10)+1} \tag{14}$$

$$\bar{i}_{Na}=0.5(E-30) \tag{15}$$

3) $\bar{i}_h=q\cdot\bar{i}_h$ (16)

$$\alpha_q=\frac{3.4\times10^{-4}(E+100)}{\exp((E+100)/4.4)-1}+4.95\times10^{-5} \tag{17}$$

$$\beta_q=\frac{5\times10^{-4}(E+40)}{1-\exp(-(E+40)/6)}+8.45\times10^{-5} \tag{18}$$

$$\bar{i}_h=0.4(E+25) \tag{19}$$

4) $i_K=p\cdot\bar{i}_K$ (20)

$$\alpha_p=\frac{9\times10^{-3}}{1+\exp(-(E+3.8)/9.71)}+6\times10^{-4} \tag{21}$$

$$\beta_p=\frac{2.25\times10^{-4}(E+40)}{\exp((E+40)/13.3)-1} \tag{22}$$

$$\bar{i}_K=\frac{0.7(\exp(0.0277(E+90))-1)}{\exp(0.0277(E+40))} \tag{23}$$

5) $i_1=0.8(1-\exp(-(E+60)/20))$ (24)

The differential equations (2) and (3) were solved by the Runge-Kutta fourth-order approximation using a digital computer (Nicolet, Model NIC-80). For the integration, the time interval of 1 msec was used for every current component except for i_{Na}. Owing to the fast kinetics of i_{Na} compared to the time-course of the action potential, the steady-state value of m and h at each membrane potential were used for calculation.

The action potential was represented by 1,024 points in the data memory and was stored on the disk for later evaluation of the action potential parameters. The calculation of both the membrane potential and the kinetic variables was started from initial values equal to the steady-state values at −60 mV. This is equivalent to the experimental condition in which the membrane potential is released from the clamp after the potential was held at −60 mV until the steady-state was reached. The solution of differential equations (2) and (3) gave a constant rhythm after about 2 sec. In the present study, the value at 2 sec was used as the initial value in every reconstruction of the membrane action potential.

The membrane current during the clamp pulse and the current-voltage relation were also calculated. Comparison of the computed curves with the experiments were very helpful in the procedure determining the empirical equations which describe the voltage dependency of the rate constants. The calculation was based on Eq. (2), and in this case the current components follow a single exponential time-course. When the model showed slight discrepancies from the experiment, the original data were re-evaluated in order to gain a better fit. The relative magnitude of each component was determined mainly from the average pattern of the current-voltage curve in the experiment.

Description of each current component.

The slow inward current, i_s: It is well established that the spontaneous activity of the S-A node cell is insensitive to TTX, while it is suppressed by an application of D 600, verapamil or manganese ion (BROOKS and LU, 1972). In agreement with these facts, in the voltage clamp experiment a rather slow inward current was recorded on depolarization from −40 mV (NOMA and IRISAWA, 1976a; NOMA *et al.*, 1977, 1980; BROWN *et al.*, 1979). This current reaches its peak amplitude at −10–0 mV and decreases with further depolarization and reverses its polarity at +30–40 mV.

The time-course of activation and inactivation was well fitted by a single exponential (NOMA *et al.*, 1980). Therefore, we adopted the formulation of BEELER and REUTER (1977) for this current,

$$i_s=d\cdot f\cdot \bar{i}_s\ ,$$

where d is the activation variable and f is the inactivation variable. The rate constants for these variables were given by Eqs. (5), (6), (7), and (8). These

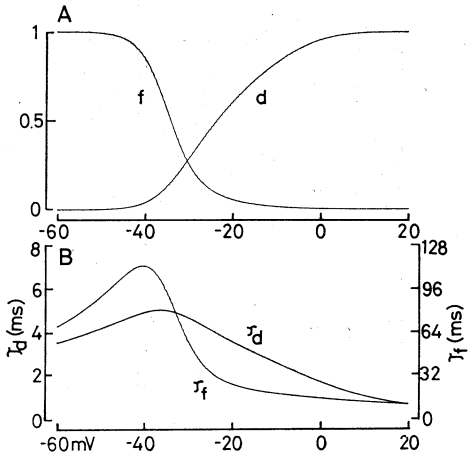

Fig. 1. Voltage relations of the steady-state degree of activation (curve d) and inactivation (curve f) for i_s and the time constant for activation (α_d) and inactivation (β_d). Note the different scale for the time constants for d (left) and f (right).

equations give the voltage relations of both the steady-state degree and the time constant for activation and inactivation of i_s in Fig. 1. During reconstruction of the voltage clamp record and the action potential, it was strongly suggested that some fraction of the i_s channel remains open in spite of the inactivation process during depolarization or removal of activation during hyperpolarization. This view has already been suggested in the ventricular muscle (REUTER, 1968). In our model, when 5% of the total number of channels remained open independent of the membrane potential (Eq. 4), the model showed a similar activity to the experiment. With this modification, 1) rather large inward current tail on repolarization even after the current change reached the steady-state during depolarization, 2) the concave (upwards) diastolic depolarization, and 3) the spontaneous action potential discharge in the absence of the time-dependent outward current (see Fig. 6) were well simulated.

i_s was separated from the total current by extrapolating the single exponential time-course of i_K to the beginning of the depolarizing clamp pulse or by subtracting the current recorded after suppressing i_s with D 600 from the control record. Figure 2 shows such an example. In a large number of records such a method gave a reversal potential of about +30–40 mV (NOMA *et al.*, 1980). Calculation of i_s using kinetic variables d and f, determined by Eqs. (5)–(8), resulted in a non-linear relation between $\bar{i}_s$ and the membrane potential, Eq. (9) (Fig. 2).

The sodium current, i_{Na}: When the membrane was hyperpolarized by carbamylcholine, the increased rate of rise of the action potential was partially depressed by an additional application of TTX (KREITNER, 1975). In the follower type S-A node cell the fast upstroke of the action potential was also depressed by

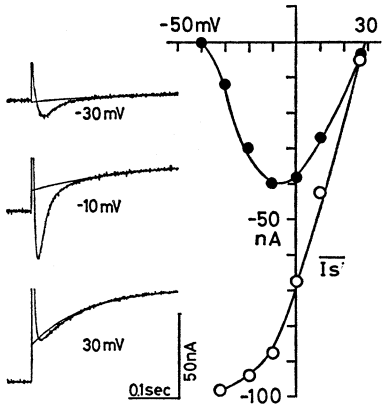

Fig. 2. Measurements of the amplitude of i_s. The experimental records are the membrane current change induced by depolarizing the clamp pulse to −30, −10, and +30 mV from the holding potential of −40 mV. Superposed smooth curves were fitted to the delayed current and extrapolated to the onset of the clamp pulse. i_s was measured as the difference between the theoretical exponential curve and the records. The right-hand graph shows the voltage relation of i_s (closed circles) measured with the same protocol as in another experiment. The open circles indicate the fully activated amplitude of the current calculated by Eqs. (4)–(8).

TTX (LIPSIUS and VASSALLE, 1978). In the voltage clamp experiment, i_{Na} was recorded when the holding potential was negative to −55 mV (NOMA *et al.*, 1977). As the voltage clamp failed to follow the fast time-course of i_{Na}, there was almost no experimental quantitative data available in the S-A node. Therefore, essentially the same description of i_{Na} as in other myocardia has been used in Eqs. (10)–(15). The reversal potential of i_{Na} was assumed as +30 mV.

The hyperpolarization-activated current, i_h: The apparent anomalous rectification of the current-voltage relation in the rabbit S-A node (NOMA and IRISAWA, 1976b; SEYAMA, 1979; YANAGIHARA and IRISAWA, 1980) and in the frog sinus venosus (BROWN *et al.*, 1977) is mainly due to i_h. i_h shows time and voltage dependency and was described by Eqs. (16)–(19). The multi-ionic nature of this current was shown in the voltage clamp experiment where replacement of Cl^- with impermeable anions, acetate, propionate (SEYAMA, 1979), or substitution of Na^+ with Tris (NOMA *et al.*, 1977) largely reduced the current amplitude. In accord with this fact the reversal potential of −25 mV was obtained (YANAGIHARA and IRISAWA, 1980).

The potassium current, i_K: i_K is the most extensively analysed compared to the other currents in the S-A node (IRISAWA, 1972; NOMA and IRISAWA, 1976b; DIFRANCESCO *et al.*, 1979; YANAGIHARA and IRISAWA, 1980). The kinetics of i_K are similar to i_{x1} in the frog sinus venosus (BROWN *et al.*, 1977) and in the ventricular muscle (BEELER and REUTER, 1970; MCDONALD and TRAUTWEIN, 1978). In these tissues a potassium current comparable to i_{K_2} in the Purkinje fiber (DECK

et al., 1964; NOBLE and TSIEN, 1968) has not been observed. i_K in the S-A node is formulated by Eqs. (20)–(23).

When the outward current is examined using rather large clamp steps, a secondary component much slower than i_K (with a time constant of a few sec) was usually observed in both the S-A node (DIFRANCESCO *et al.*, 1979) and the frog sinus (BROWN *et al.*, 1977). This component was neglected in the present model, because this secondary component is not significantly large as far as the clamp pulse is of comparable size to the action potential. Discrepancy due to lack of the slow component in the simulation of the voltage clamp record will be discussed later in the present study.

The leak current, i_l: It was impossible to measure the magnitude of the time-independent leak current directly from the current trace in the voltage clamp experiment, because the current jump at the onset of the clamp pulse is also due to time-dependent components. Therefore, we have estimated the approximate amplitude of the leak current from the difference between the computed total amplitude of the above 4 time-dependent components and the experimental current-voltage relation in the steady-state. Equation (24) simulated i_l.

Relative amplitude of individual components.

In the present model 5 current components, i_s, i_{Na}, i_h, i_K, and i_l were used. These current components were analysed in different preparations and thus, it was necessary to determine the relative amplitude of each component. The amplitude of i_s was initially determined by adjusting the maximum rate of rise of the action potential to the average value of about 4 V/sec through 1 μF/cm^2 membrane capacitance. The amplitude of the delayed current on depolarization was used to determine i_K and that during hyperpolarization was used for i_h. The amplitude of i_{Na} was determined by fitting the current record in Fig. 1 by NOMA *et al.* (1977).

RESULTS

Membrane current during the voltage clamp pulse

In Fig. 3 the computed currents induced by clamp pulses were compared with the corresponding record in the experiment by NOMA and IRISAWA (1976a) (see for general pattern of i_s also NOMA *et al.*, 1977, 1980; NOMA and TRAUTWEIN, 1978). The calculated current was scaled so as to give an amplitude equal to i_s at 0 mV in the experiment. Generally, the time-course and amplitude of the current are similar to the experimental ones. An obvious discrepancy is mainly caused by the capacitive current in the experiment which is not included in the model calculation. The activation time-course of i_s on depolarization to -30 mV and 0 mV are little affected by the capacitive current, but at $+20$ mV the trace within 5–10 msec is largely due to the capacitive current and the peak amplitude is smaller than that in the computed trace. Thus, in the experiment measuring the

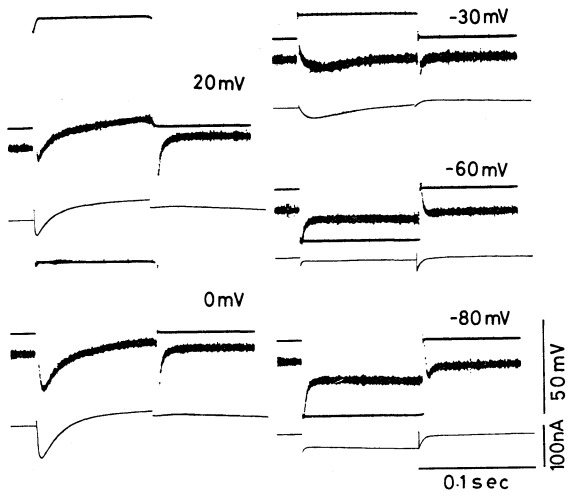

Fig. 3. Comparison of the reconstructed current traces with the experimental ones at various clamp potentials. The experimental traces were the same experiment as that of NOMA and IRISAWA (1976, Fig. 7).

activation of i_s the interference by the capacitive current must be avoided by subtraction of two currents recorded with identical pulses before and during suppression of i_s with its blocker (NOMA *et al.*, 1980). At positive potential i_K is significantly activated and an outward current tail is evident on repolarization. During hyperpolarization, the activation of i_h is not significant because of the short duration of the pulse and on clamping back to the holding potential, the activation of i_s was not clearly recorded in the experiment.

The current voltage relationship

The validity of the present model was also tested by reconstructing the current-voltage relationship. In Fig. 4 the current voltage curves (*I-V* curve) at 0, 5, and 1,000 msec were calculated. The *I-V* curve at 0 msec (middle trace at around 0 mV) is mainly attributable to the time-independent i_1 and the steady conductance of i_s at the holding potential of −40 mV. At 5 msec activation of i_s is obvious positive to −40 mV (bottom curve). At 1 sec two delayed currents, i_K on depolarization (top curve) and i_h on hyperpolarization (bottom curve at around −80 mV), are the main components contributing to the *I-V* curve. Steady-state conductance of i_s causes two effects on the *I-V* curve: 1) The small hump at around −30 mV in the *I-V* curve at 1 sec is caused by the overlapping of the steady-state activation curve and inactivation curve (Fig. 1). 2) On hyperpolarization the steady-state conductance of i_s at the holding potential rapidly deactivated and the *I-V* curve shifted upwards from 0 to 5 msec.

In the spontaneously beating S-A node cell, the resting potential can be defined by the potential where the steady-state *I-V* curve intersects the voltage

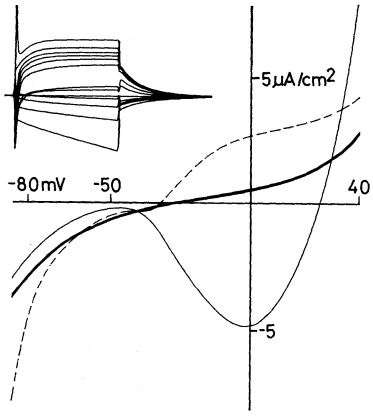

Fig. 4. Reconstruction of the current-voltage relationship at 0 msec (thick line), 5 msec (thin line) and 1 sec (broken line) after the onset of the clamp pulse from the holding potential of −40 mV.

axis. In the present model the resting potential was −31.7 mV. This value is slightly positive compared to the experimentally obtained values which were around −37 mV (NOMA and IRISAWA, 1975b).

Spontaneous action potential

The model showed a spontaneous action potential as shown in the top curve of Fig. 5A. Changes in current components (i_K, i_s, i_h, i_{Na}, i_l) and the total current (I) underlying the action potential are shown. The maximum diastolic potential was −62.4 mV, overshoot +20.7 mV, duration 80 msec at −20 mV and the maximum rate of rise was 3.8 V/sec with a frequency of discharge of 171/min. A large fraction of the membrane current is provided by i_K, i_s, and i_l. The amplitudes of i_h and i_{Na} are much smaller compared to these three major current components. The rising phase of the action potential is due to the transient flow of i_s and repolarization is caused by the combination of decay in i_s and increase in i_K.

The model indicated a rather large contribution of i_s to the pacemaker depolarization in the S-A node than in the Purkinje fiber. During the pacemaker potential i_K decreased only slightly, but i_s significantly increased. For i_K the kinetic variable p is continuously decreasing (Fig. 5B), but this change is almost neutralized by the opposite change in $\bar{i}_K$. On the other hand, the recovery of f from nearly zero at the end of the action potential to 0.8–0.9 during the diastolic period caused a gradual increase in i_s (Fig. 5B). During diastole the outward leak current gradually increased, resulting in a nearly constant inward net current during diastole. Thus, the slope of the diastolic depolarization is almost constant.

Pacemaker depolarization dependent on i_s was strongly suggested by the ex-

periments examining the effects of Ba^{2+} on the membrane current of the S-A node cell. In the presence of 5 mM Ba^{2+}, i_K was nearly completely depressed and the membrane depolarized to about −10 mV. Under this condition, the application of a constant hyperpolarizing current resumed the pacemaker activity (YANAGIHARA and IRISAWA, 1980). The analogous condition was simulated by substituting i_K with various magnitudes of constant out-going current. In the absence of i_K the model depolarized to −9 mV. As the added current was increased from 0.25 to 0.5 $\mu A/cm^2$, the oscillatory current grew to full size action potential and further hyperpolarization completely abolished the spontaneous activity (Fig. 6). Under this condition the pacemaker depolarization is simply caused by

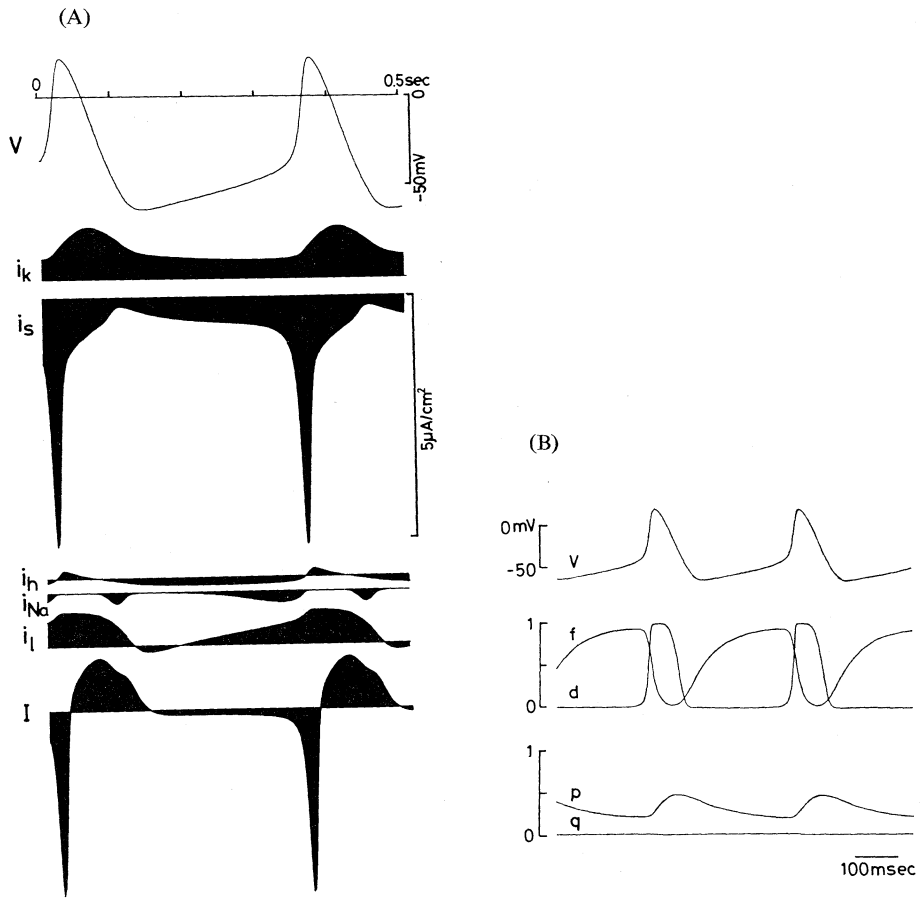

Fig. 5. A: Ionic mechanism for the spontaneous action potential discharge. *V*, the membrane potential; i_K, the potassium current; i_s, the slow inward current; i_h, the hyperpolarization-activated current; i_{Na}, sodium current; i_l, the leak current; *I*, total current. Note the smaller decrease in i_K during diastole compared to i_s and i_l. B: Changes in the kinetic variables for i_s, i_K, and i_h during the spontaneous action potential.

a time-dependent increase in i_s.

Modification of rhythm by epinephrine and acetylcholine

Epinephrine increases i_s, i_K and i_h (BROWN *et al.*, 1979) and this increase was attributed to the amplitude of $\bar{i}_s$, $\bar{i}_K$, and $\bar{i}_h$ by average factors of 1.3, 1.1, and 1.2 at 5.5×10 M, respectively (NOMA *et al.*, 1980). When we increased only i_K by a

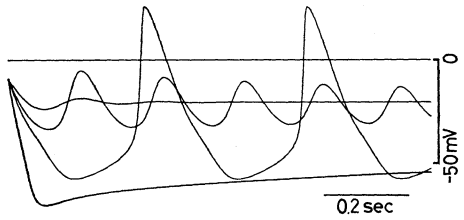

Fig. 6. Resumption of the spontaneous rhythm by constant hyperpolarizing currents in a model depolarized to −9 mV by reducing i_K to 0. At the beginning of the traces outward currents of 0.25, 0.4, 0.5, and 1 μA/cm^2 were added to the membrane current throughout the trace. The protocol simulates the activity of the S-A node under the effect of i_K-blocker such as Ba^{2+}. Top line indicates 0 potential level.

factor of 1.1, the spontaneous frequency of the model decreased from 171 to 165/min. When i_s increased by a factor of 1.3, spontaneous frequency increased from 171 to 199/min, while when i_h increased 1.2 times, heart rate only increased to 174/min. Therefore, the chronotropic effect of epinephrine is largely dependent on an increase in i_s. Figure 7-1 simulates the effect of epinephrine, the maximum rate of rise of the action potential increased from 3.8 to 5.2 V/sec, the overshoot increased by 3.0 mV, while the maximum diastolic potential and the duration remained constant. Thus, the model well simulated the epinephrine effect on the activity of the S-A node cell.

Recently, the kinetic property of the ACh-induced K current (i_{ACh}) was examined in the rabbit S-A node cell (NOMA and TRAUTWEIN, 1978; NOMA *et al.*, 1979a, b; OSTERRIEDER *et al.*, 1980). According to these studies, the opening (α) and closing rate constants (β) are given by,

$$\alpha_{ACh}=\frac{12.32\times10^{-3}}{1+(4.2\times10^{-6}/A)}\,, \tag{25}$$

$$\beta_{ACh}=0.01\exp(0.0133\times(E+40))\,, \tag{26}$$

where A is the concentration of ACh. The amplitude of i_{ACh} under full activation is,

$$i_{ACh}=0.27(E+90)\,. \tag{27}$$

Using these equations the ACh-induced current was incorporated in the present model. In the computation in Fig. 7-2, it was assumed that 3 concentrations of

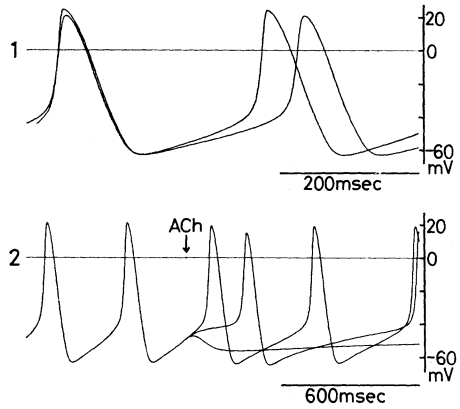

Fig. 7. Modification of the spontaneous rhythm by epinephrine (1) and by acetylcholine (2). In 1, the action potential with a higher overshoot in epinephrine solution was superposed on the control. In 2, at the arrow i_{ACh} was added which was activated by 5×10^{-8}, 10^{-7}, and 2×10^{-7} M ACh. The effect of ACh in this calculation corresponds to the experiments in the presence of choline-esterase blocker.

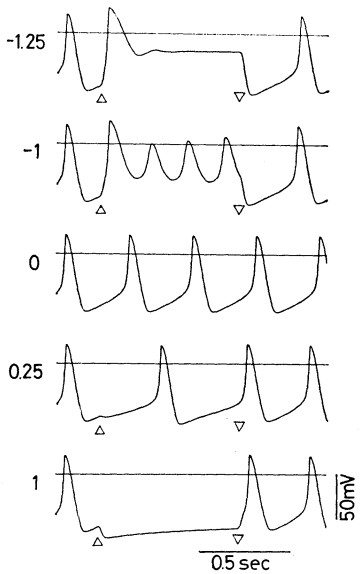

Fig. 8. Modification of the spontaneous rhythm by adding various magnitudes of external current to the model circuit. The numerals left of the records indicate the magnitude of the applied current in $\mu A/cm^2$. The switch on and off of the current pulse are indicated by triangles.

ACh were applied at the arrow. The spontaneous frequency decreased from 173/min in normal Tyrode to 132 and 79/min at 5×10^{-8} and 10^{-7} M, respectively, while at 2×10^{-7} M, it ceased. These results agree well with the experiment (DEL

CASTILLO and KATZ, 1955; TRAUTWEIN and DUDEL, 1958). At 2×10^{-7} M ACh, the hyperpolarization within about 150 msec is caused by a gradual activaton of i_{ACh} with a time constant of about 110 msec and the following slow depolarization is due to activation of i_h.

Modification of rhythm by external current application

The model also well simulated the finding that the frequency of the spontaneous action potential can be controlled by applying current (NOMA and IRISAWA, 1974). In Fig. 8, an application of outward-going current increased the frequency, while an application of inward-going current reduced the frequency. Spontaneous discharge was observed at the potential range between −19 and −60 mV of the maximum diastolic potential.

DISCUSSION

The present study using the Hodgkin-Huxley type model elucidated the major role of i_s in generating both the action potential and the pacemaker depolarization. This model well simulated the electrical responses of the S-A node cell to various experimental conditions.

In the present study, the typical pattern of the S-A node action potential was modelled. The action potentials in different parts of the S-A node region always showed quantitative differences in the maximum rate of depolarization, amplitude and the maximum diastolic potential (SANO and YAMAGISHI, 1965; SEYAMA, 1976). One reason for these variations is the conduction of the action potential. Primary pacemaker cell shows a low take-off potential and thus the rate of rise may be slowed down and the follower cells have a rather high rate of rise. However, even in a small preparation, where no conduction occurs, we frequently observed certain differences in the maximum rate of rise and the amplitude of the action potential. It is unlikely that different cells have different current systems, but we assume that a slight difference occurs in the relative amplitude of the current systems and in the voltage relation of the kinetic parameters. Thus, a larger action potential in some cells especially those located close to the crista terminalis may be simulated by increasing i_s and i_K.

Subthreshold oscillation in the S-A node cell may be characterized by its sinusoidal shape with a similar frequency to the spontaneous action potential (WEST, 1964). Such oscillation was observed in a low Na solution or a low K solution or on releasing the membrane potential from the "resting potential level" by switching off the voltage clamp. When $\bar{i}_s$ was decreased in the model to simulate a low Na condition, the frequency of oscillation was reduced and the shape of the potential was like a depressed action potential. Oscillation that occurred on releasing the voltage clamp was simulated by the present model (Fig. 9A). The steeper repolarization after the first hump (in Fig. 9A) than those in the experimental record (NOMA and IRISAWA, 1975b) was improved by a small change in

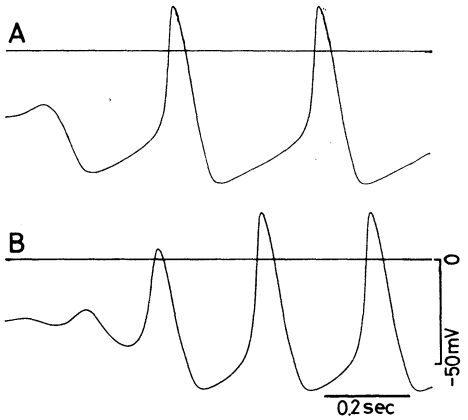

Fig. 9. Reconstruction of the oscillatory potential after releasing the membrane potential from the clamp at −30 mV. A: The control model shows rather quick hyperpolarization after an initial slight depolarization. This was due to rapid decrease of i_s caused by a decrease in d. B: The model was slightly modified only for the rate constant, α_d.

$$\alpha_d = \frac{1.045\times10^{-2}(E+35)}{1-\exp(-(E+35)/5)} + \frac{3.125\times10^{-2}E}{1-\exp(-E/4.8)}$$

The resting potential of this modified model was −29.8 mv.

the voltage relation of kinetic variable d (Fig. 9B).

The model failed to simulate the response of the S-A node to D 600. The model hyperpolarized by approximately 20 mV in the absence of i_s. In the experiment we never observed such a large hyperpolarization on application of D 600, but most preparations depolarized by several mV. Even if we assume a concomitant slight decrease of i_K (KASS and TSIEN, 1975) the model showed a significantly large hyperpolarization. Several mechanisms underlying the electrical activity of the cell were ignored in the present model; the electrogenic Na pump (NOMA and IRISAWA, 1975a), control of the potassium conductance by intracellular Ca (ISENBERG, 1977) and the Na-Ca exchange mechanism (HORACKOVA and VASSORT, 1979). These factors might have caused the above discrepancy. However, at present we cannot definitely attribute this discrepancy to any of these mechanisms.

The slower component of the outward current than i_K is a rather regular finding in the S-A node as in other tissues (for review, see TRAUTWEIN, 1973). In the present model we did not include this current as an independent current system, because of its extremely slow time-course and unknown nature. This caused an obvious discrepancy in the current pattern in the voltage clamp; the tail current returned completely to the holding current level already 1 sec after the clamp pulse, which was not the case in the experiment. In normal activity, however, this component may act similarly to the time-independent current because of the slow time constant compared to the spontaneous frequency. The

role of the slow component of the outward current may become important when the cell is overdriven. The cumulative activation of this current during succeeding action potentials may hyperpolarize the cell and act to decelerate the spontaneous activity.

The present model for the S-A node activity suggested a large contribution of i_s and i_1. Experimentally, however, these two currents are most difficult to quantify, because of limited time resolution of the voltage clamp and lack of selective blockers of the current components. Therefore, the present model cannot give a final answer of the ionic mechanism of the S-A node pacemaker activity, but the present study disclosed the following two characteristics of these currents. The window current of i_s, given by the product of d_∞ and f_∞ cannot be larger than the present model; a larger window current results in a larger inward hump on the steady-state *I-V* curve which is far from the experimental findings. We did not separate the time-independent leak current into several components in the present study, but its total amplitude should rectify in the inward direction.

We thank Dr. I. Seyama for his critical comments through this study.

REFERENCES

BEELER, G. W., Jr. and REUTER, H. (1970) Voltage clamp experiments on ventricular myocardial fibres. *J. Physiol. (Lond.)*, **207**: 167–190.

BEELER, G. W., Jr. and REUTER, H. (1977) Reconstruction of the action potential of ventricular myocardial fibres. *J. Physiol. (Lond.)*, **268**: 177–210.

BROOKS, C. McC. and LU, H. H. (1972) The Sinoatrial Pacemaker of the Heart, Charles C. Thomas Publ., Springfield, Ill.

BROWN, H. F., GILES, W., and NOBLE, S. J. (1977) Membrane currents underlying activity in frog sinus venosus. *J. Physiol. (Lond.)*, **271**: 783–816.

BROWN, H. F., DIFRANCESCO, D., and NOBLE, S. J. (1979) How does adrenaline accelerate the heart? *Nature*, **280**: 235–236.

DECK, K. A., KERN, R., and TRAUTWEIN, W. (1964) Voltage clamp technique in mammalian cardiac fibers. *Pflügers Arch. Ges. Physiol.*, **280**: 50–62.

DEL CASTILLO, J. and KATZ, B. (1955) Production of membrane potential changes in the frog's heart by inhibitory nerve impulses. *Nature*, **175**: 1035.

DIFRANCESCO, D., NOMA, A., and TRAUTWEIN, W. (1979) Kinetics and magnitude of the time-dependent K current in the rabbit S-A node: Effect of external potassium. *Pflügers Arch.*, **381**: 271–279.

DRAPER, M. H. and WEIDMANN, S. (1951) Cardiac resting and action potentials recorded with an intracellular electrode. *J. Physiol. (Lond.)*, **115**: 74–94.

HODGKIN, A. L. and HUXLEY, A. F. (1952) A quantitative description of membrane current and its application to conduction of excitation in nerve. *J. Physiol. (Lond.)*, **117**: 500–544.

HORACKOVA, M. and VASSORT, G. (1979) Sodium-calcium exchange in regulation of cardiac contractility. Evidence for an electrogenic, voltage-dependent mechanism. *J. Gen. Physiol.*, **73**: 403–424.

IRISAWA, H. (1972) Electrical activity of rabbit sino-atrial node as studied by a double sucrose gap method. *In*: Proceedings of the Satellite Symposium of the XXVth International Congress of Physiological Sciences, ed. by RIJLANT, P. Presses Academiques Europeenes, Bruxelles.

IRISAWA, H. (1978) Comparative physiology of the cardiac pacemaker mechanism. *Physiol. Rev.*, **58**: 461–498.

ISENBERG, G. (1977) Cardiac Purkinje fibres $[Ca^{++}]_o$ control steady state potassium conductance. *Pflügers Arch.*, **371**: 71–76.

KASS, R. S. and TSIEN, R. W. (1975) Multiple effects of calcium antagonists on plateau currents in cardiac Purkinje fibers. *J. Gen. Physiol.*, **66**: 169–192.

KREITNER, D. (1975) Evidence for the existence of a rapid sodium channel in the membrane of rabbit sinoatrial cells. *J. Mol. Cell. Cardiol.*, **7**: 655–662.

LIPSIUS, S. L. and VASSALLE, M. (1978) Dual excitatory channels in the sinus node. *J. Mol. Cell. Cardiol.*, **10**: 753–767.

MCALLISTER, R. E., NOBLE, D., and TSIEN, W. (1975) Reconstruction of the electrical activity of cardiac Purkinje fibres. *J. Physiol. (Lond.)*, **251**: 1–59.

MCDONALD, T. F. and TRAUTWEIN, W. (1978) The potassium current underlying delayed rectification in cat ventricular muscle. *J. Physiol. (Lond.)*, **274**: 217–246.

NOBLE, D. and TSIEN, R. W. (1968) The kinetics and rectifier properties of the slow potassium current in cardiac Purkinje fibres. *J. Physiol. (Lond.)*, **195**: 185–214.

NOMA, A. and IRISAWA, H. (1974) The effect of sodium ion on the initial phase of the sinoatrial pacemaker action potential in rabbits. *Jpn. J. Physiol.*, **24**: 617–632.

NOMA, A. and IRISAWA, H. (1975a) Contribution of an electrogenic sodium pump to the membrane potential in rabbit sinoatrial node cells. *Pflügers Arch.*, **358**: 289–301.

NOMA, A. and IRISAWA, H. (1975b) Effects of Na^+ and K^+ on the resting membrane potential of the rabbit sinoatrial node cells. *Jpn. J. Physiol.*, **25**: 287–302.

NOMA, A. and IRISAWA, H. (1976a) Membrane currents in the rabbit sinoatrial node cell as studied by the double microelectrode method. *Pflügers Arch.*, **364**: 45–52.

NOMA, A. and IRISAWA, H. (1976b) A time- and voltage-dependent potassium current in the rabbit sinoatrial node cell. *Pflügers Arch.*, **366**: 251–258.

NOMA, A., OSTERRIEDER, W., and TRAUTWEIN, W. (1979a) The effect of external potassium on the elementary conductance of the ACh-induced potassium channel in the sino-atrial node. *Pflügers Arch.*, **381**: 263–269.

NOMA, A., PEPER, K., and TRAUTWEIN, W. (1979b) Acetylcholine-induced potassium current fluctuations in the rabbit sino-atrial node. *Pflügers Arch.*, **381**: 255–262.

NOMA, A. and TRAUTWEIN, W. (1978) Relaxation of the ACh-induced potassium current in the rabbit sinoatrial node cell. *Pflügers Arch.*, **377**: 193–200.

NOMA, A., YANAGIHARA, K., and IRISAWA, H. (1977) Inward current of the rabbit sinoatrial node cell. *Pflügers Arch.*, **372**: 43–51.

NOMA, A., KOTAKE, H., and IRISAWA, H. (1980) Slow inward current and its role mediating chronotropic effect of epinephrine. *Pflügers Arch.*, **388**: 1–9.

OSTERRIEDER, W., NOMA, A., and TRAUTWEIN, W. (1980) On the kinetics of the potassium channel activated by acetylcholine in the S-A node of the rabbit heart. *Pflügers Arch.*, **386**: 101–109.

REUTER, H. (1968) Slow inactivation of currents in cardiac Purkinje fibres. *J. Physiol. (Lond.)*, **197**: 233–253.

SANO, T. and YAMAGISHI, S. (1965) Spread of excitation from the sinus node. *Circ. Res.*, **16**: 423–430.

SEYAMA, I. (1979) Characteristics of the anion channel in the sino-atrial node cell of the rabbit. *J. Physiol. (Lond.)*, **294**: 447–460.

SEYAMA, I. (1976) Characteristics of the rectifying properties of the sino-atrial node cell of the rabbit. *J. Physiol. (Lond.)*, **255**: 379–397.

TRAUTWEIN, W. (1973) Membrane currents in cardiac muscle fibers. *Physiol. Rev.*, **53**: 793–835.

TRAUTWEIN, W. and DUDEL, J. (1958) Zum Mechanismus der Membranwirkung des Acetylcholin an der Herzmuskelfaser. *Pflügers Arch. Ges. Physiol.*, **266**: 324–334.

TRAUTWEIN, W. and ZINK, K. (1952) Über Membran- und Aktionspotentiale einzelner Myokardfasern des Kalt- und Warmbluterherzens. *Pflügers Arch. Ges. Physiol.*, **256**: 68–84.

YANAGIHARA, K. and IRISAWA, H. (1980) Inward current activated during hyperpolarization in the rabbit sinoatrial node cell. *Pflügers Arch.*, **385**: 11–19.

YANAGIHARA, K. and IRISAWA, H. (1980) Potassium current during the pacemaker depolarization in rabbit sinoatrial node cell. *Pflügers Arch.*, in press.

WEIDMANN, S. (1955) The effect of the cardiac membrane potential on the rapid availability of the sodium-carrying system. *J. Physiol. (Lond.)*, **127**: 213–224.

WEST, T. C. (1955) Ultramicroelectrode recording from the cardiac pacemaker. *J. Pharmac. Exp. Ther.*, **115**: 283–290.

WEST, T. C. (1964) Effects of chronotropic influences on subthreshold oscillations in the sinoatrial node. *In*: The Specialized Tissues of the Heart, ed. by PAES, DE CARVALHO, DEMELLO, W. C., and HOFFMAN, B. F. Elsevier, New York, pp. 81–94.